

Particle advection by turbulent bores—Orientation effects

Catherine M. Petroff¹, Andrew L. Moore², and Halldor Árnason¹

¹*Department of Civil Engineering, University of Washington, Seattle, Washington, U.S.A.*

²*Disaster Control Research Center, Tohoku University, Aoba, Sendai, Japan*

Abstract. Hydraulic reconstruction of paleotsunamis hinges on understanding the relationship between bore size and particle advection length. Although previous studies have shown that a relationship does exist between bore size, particle size, and particle advection length, none have studied the relationship between particle shape, initial orientation and advection length.

We performed experiments with nine aluminum rectangular prisms and five aluminum cubes to determine the effect of shape on advection distance. The prisms were sized so that particle volume remained constant while the volume of the cubes varied. Bore height and velocity were held constant. Prisms were placed so that a different face was facing the flow for each experiment.

Our results show that, for constant particle volume and density, the advection distance is a function of the axis length along the direction of flow. As the length of the particle axis in the flow direction increases, its advection length decreases. For example, the advection length of a prism with a given plane facing the flow is determined by the length of the third axis. These results suggest that tsunami hydraulic reconstructions based on irregularly shaped objects may depend on the shape factor and on the original orientation of the objects.

1. Introduction

A common feature of areas struck by tsunamis is the presence of blocks of debris, such as building rubble or coral reef debris, that were moved by the waves (Dominey-Howes *et al.*, 2000; Makino, 1980; Nakata and Kawana, 1993; Simpkin and Fiske, 1983; Yamashita, 1995; Yeh *et al.*, 1993). This large grain-size material may be the only geologic record of ancient tsunamis in coastal areas where sand sheets were not permanently deposited. The tsunami history of some tsunami-prone areas may be clarified by quantifying the relationship between the distance traveled by blocks of debris and the size of the wave that moved them.

2. Force Analysis

Two of the forces responsible for determining the advection length of a particle are the hydraulic force on the particle in the direction of transport, and the submerged weight of the particle. The submerged weight of the particle (F_W) is simply determined as:

$$F_W = (\rho_s - \rho_f)gV \quad (1)$$

¹University of Washington, Department of Civil and Environmental Engineering, Box 352700, Seattle, WA 98195-2700, U.S.A. (cpetroff@u.washington.edu, harnason@u.washington.edu)

²Tsunami Engineering Laboratory, Disaster Control Research Center, Graduate School of Engineering, Tohoku University, Aobayama 06, Sendai 980-8579, Japan (moore@tsunami2.civil.tohoku.ac.jp)

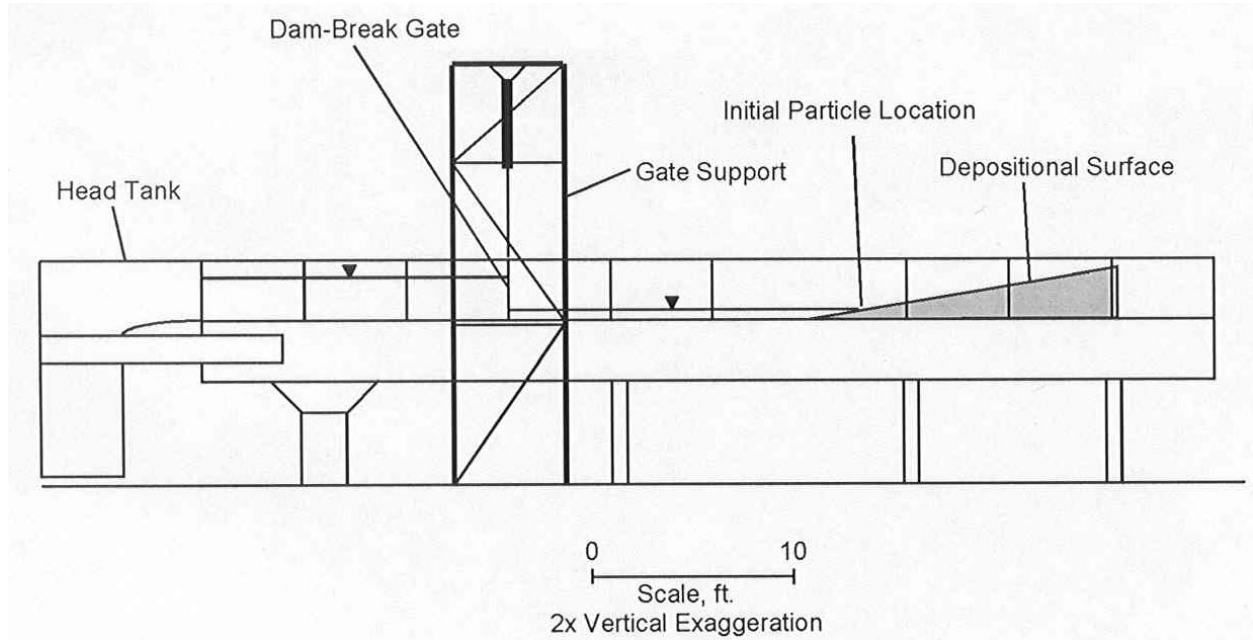


Figure 1: Schematic drawing of the wave tank used for the experiments. For all experiments, the depth of water between the gate and the depositional surface was 2 cm and the maximum possible advection length was 354 cm.

where ρ_s is the density of the particle, ρ_f is the density of the fluid, g is the acceleration of gravity, and \forall is the volume of the particle.

For bores, the average velocity in the direction of travel is much greater than average vertical or cross-stream velocity components. The in-line force on a particle has been expressed by O'Brien and Morison (1952) to be the sum of a drag term proportional to the square of the free stream velocity, and an inertial term proportional to the instantaneous acceleration:

$$F_D = \frac{1}{2}\rho_f C_D A u^2 + \rho_f C_M \forall \frac{\partial u}{\partial t} \quad (2)$$

where C_D is the drag coefficient, A is the projected area of the particle in the flow direction, u is the cross section averaged flow velocity, $\partial u / \partial t$ is the instantaneous flow acceleration, and C_M is the inertia coefficient.

For fully turbulent flow, viscous forces are negligible, so we can postulate that advection length scales with the ratio of the buoyant weight of the particle to the in-line force on the particle:

$$\frac{F_W}{F_D} = \frac{(\rho_s - \rho_f)g\forall}{\frac{1}{2}\rho_f C_D A u^2 + \rho_f C_M \forall \frac{\partial u}{\partial t}} \quad (3)$$

The coefficient of inertia is difficult to estimate for natural particles and the real impact force on boulders during tsunamis includes effects that do not scale well in lab experiments. Additionally, both drag and inertial coefficients are strongly time-dependent for unsteady flows such as bores. Our experiment observations showed that for relatively large cubes, cubes near

the larger limit of what can be transported by a bore, the cubes are not moved during the initial, maximum acceleration, portion of the bore, but rather after the establishment of maximum velocity. Although the bore front is a region of strong acceleration and consequently high inertial force, Noji *et al.* (1985) report from numerical simulations that the force exerted on a cube by a bore reaches a maximum at the maximum velocity, rather than at the maximum acceleration. We observed in our experiments that the particles were entrained after passage of the bore head, in a region of the bore with relatively stable velocity. If the inertial force is not sufficient to move a particle, the first motion occurs well after the zone of acceleration at the bore head because a finite amount of time is required to establish velocity profiles in the flow, and consequently full hydraulic drag on the cube. For our experiments we can neglect the inertial term in (3), and simplify the force ratio to:

$$\frac{F_W}{F_D} = \frac{2(\rho_s - \rho_f)g\forall}{\rho_f C_D A u^2} \quad (4)$$

Because ρ_f , ρ_s , and u were held constant for our experiments, this force ratio varies as:

$$\frac{F_W}{F_D} = \alpha \frac{X}{C_D}, \text{ where } \alpha = \frac{2(\rho_s - \rho_f)g}{\rho_f u^2} \quad (5)$$

where X is particle axis length in the direction of flow.

3. Experimental Procedures

The experiments were made in a 20-m long wave tank fitted with a pneumatically activated gate 7 m from the head tank (Fig. 1). The tank is 60 cm wide and 45 cm deep, with a stainless steel bottom plane to within ± 1 mm. A pneumatic piston lifts the gate at 2 m/s, allowing it to clear the top of the tank in 0.2 s.

On the downstream end of the tank was a wooden beach with a slope of 0.1. The beach was faired to the tank floor with silicone sealant and up to the 5 cm elevation had a stainless steel toe. From 5 cm to the maximum beach height at 35.4 cm, the beach was roughened with coarse sand ($D_{50} = 0.84$ mm, $\sigma_i = 0.436\Phi$) cemented to the wooden surface.

The “particles” used in these experiments were cubes and rectangular prisms made of aluminum (Table 1). For particles α through ι the notations “A,” “B,” and “C” refer to the longest, intermediate, and shortest orthogonal axes of the particle, respectively. The rectangular prisms were proportioned so that their volume corresponded closely to the volume of a 16-mm cube. For each experiment, water was impounded to a depth of 30 cm behind the gate, while 2 cm of water remained in front of the gate. This resulted in a bore height of 6.5 cm and a peak flow velocity of approximately 155 cm/s at the beach sustained for over 3 s. For cubic particles, five particles were placed with their “seaward” edge at the waterline, and the experiment repeated six times, for a total of 30 particle advections. For rectangular prisms, three of

Table 1: Dimensions of particles used in this study.

Name	A axis (cm)	B axis (cm)	C axis (cm)	Density (g/cm ³)	Volume (cm ³)	Shape Factor
8 mm	0.80	0.80	0.80	2.717	0.512	1
12 mm	1.20	1.20	1.20	2.717	1.728	1
16 mm	1.60	1.60	1.60	2.717	4.096	1
20 mm	2.00	2.00	2.00	2.717	8.000	1
24 mm	2.40	2.40	2.40	2.717	13.824	1
α	2.15	1.60	1.19	2.717	4.094	0.64
β	2.39	1.60	1.07	2.717	4.092	0.55
γ	3.29	1.17	1.06	2.717	4.081	0.54
δ	3.14	1.28	1.02	2.717	4.100	0.51
ε	2.95	1.42	1.00	2.717	4.189	0.49
ζ	2.69	1.60	0.95	2.717	4.088	0.46
η	2.43	1.84	0.92	2.717	4.114	0.43
θ	3.08	1.60	0.84	2.717	4.140	0.38
ι	3.66	1.60	0.72	2.717	4.216	0.30

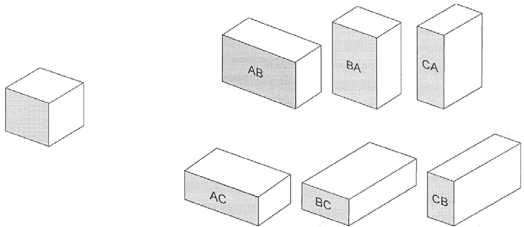
each particle were placed at the waterline, and the experiment repeated 5 times for a total of 15 particle advectations. As shown in Table 2, six different orientations were used for prism experiments—each face normal to the flow, with both the long and short orthogonal side down.

The advection distance of each particle was recorded with a super-8 video recorder mounted on a moveable bracket over the tank and oriented parallel to the beach. Marks placed every centimeter along the centerline and each edge of the beach provided calibration for the camera view.

4. Results and Discussion

For a given particle with a fixed initial orientation, the advection length in repeated experiments is highly variable (Fig. 2). The results for three orientations of the prism “ α ” are shown in a histogram. The longest and shortest advection distances vary by as much as 29% from the median advection distance. In addition, Fig. 2 shows that each orientation has a different distribution and consequently a different mean advection distance.

Table 2: Experiment parameters and orientations of particles used in this study.

	Bore height = 6.5 cm		Cubes:		Rectangular prisms:	
	Beach slope = 1/10		8 mm–24 mm		$\alpha - \iota$	
	Still water depth = 2 cm		30 runs each		15 runs at each orientation	
Orientation and Face Normal to Flow						

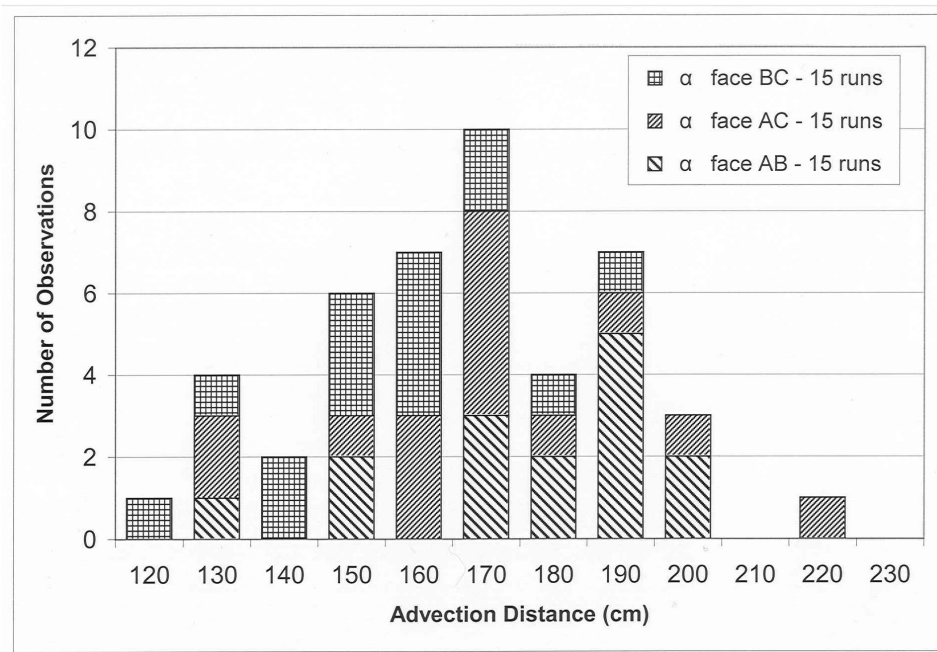


Figure 2: Histogram of measured advection lengths for particle α , faces AB, AC, and BC, moved by a 6.5 cm high bore with a peak horizontal velocity of approximately 155 cm/s.

Figure 3 demonstrates that the median advection length of a particle shows a strong correlation with particle length in the direction of flow. This figure was obtained by plotting the median advection distances of the cubes and the prisms in all six particle orientations against X/C_D , the length of the flow parallel axis divided by an estimated drag coefficient. Drag coefficients for each particle orientation were estimated by using measured values for cubes and plates of finite dimensions and by adjusting for particle length by using observations of drag on flow parallel cylinders of varying length (Rouse, 1950; Blevins, 1984). The resulting drag coefficients varied by less than 10%. Figure 3 suggests that particles with their smallest face normal to the bore tend to advect shorter distances than a cube of similar volume: the advection distance of particle “ ι ” in the BC and CB orientations is between that of a 20-mm and a 24-mm cube, whereas its volume is close to that of the 16-mm cube. Prisms placed with their largest face to the flow tend to travel slightly farther than a cube of equivalent volume. Figure 3 also shows that particles with the lowest shape factors have large variations in behavior due to orientation while particles with shape factors closer to that of a cube have smaller variations.

Since the effects of the variation of a free stream drag coefficient have been accounted for in the analysis, it is likely that the differences seen in advection length are due to particle rotation and motion during movement. This force ratio of weight to drag in (3) implicitly assumes that particles remain in their original position during advection. Visual observation of the

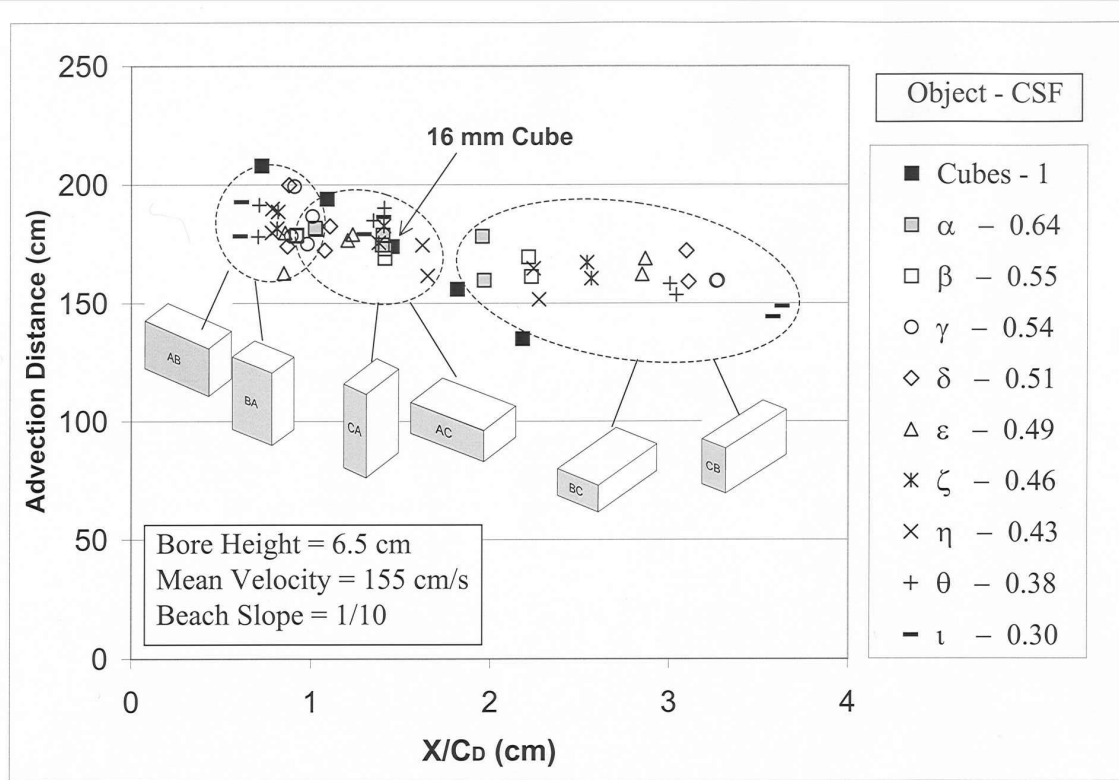


Figure 3: Median advection distance vs. flow-direction particle length divided by drag coefficient for 8-, 12-, 16-, 20-, and 24-mm cubes and rectangular prisms “ α ” through “ τ .”

particles during advection, however, shows that they rotate so that their longest axis is normal to the flow, then rotate or roll about that axis. The CB or BC initial orientation of a particle appears to impede transition to this orientation for enough time to shorten its total length of travel. It is evident that the exact motion of irregular particles as they advect influences their advection distance.

In paleohydraulic reconstructions of tsunamis, original particle orientation is generally unknown. We took the median advection length for each particle without regard to orientation, and plotted it on the same axes as before, but using the mean axis length, \overline{X} , in place of the flow-parallel axis length, where:

$$\overline{X} = \sqrt[3]{abc} \quad (6)$$

and a , b , and c are the major, intermediate, and minor axis lengths. The average drag coefficient was calculated using the coefficients for all six orientations. When averaged, the behavior of the prisms is indistinguishable from that of the 16-mm cube (Fig. 4).

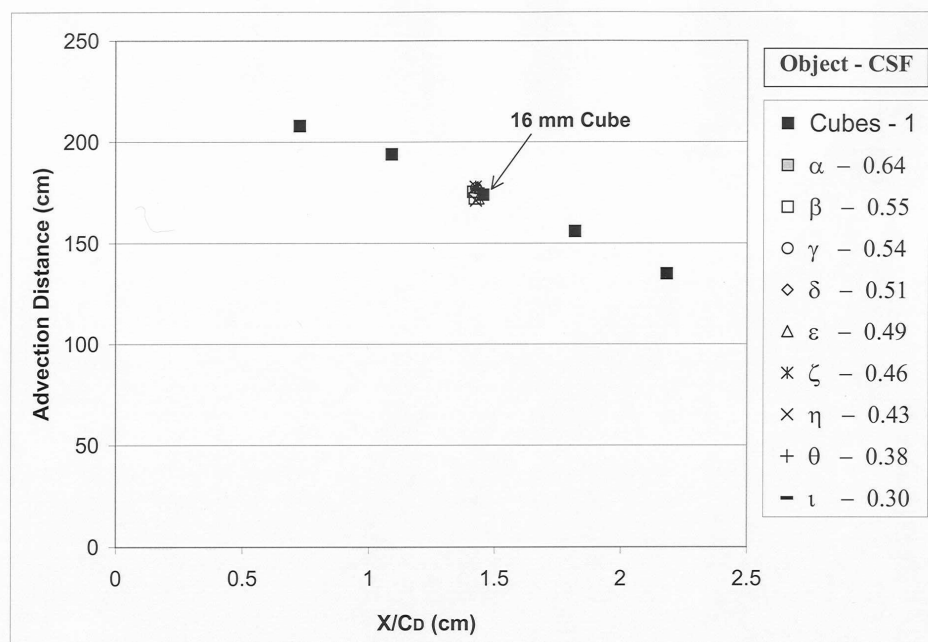


Figure 4: Median advection distance averaged over all six particle orientations vs. average particle axis length divided by average drag coefficient for 8-, 12-, 16-, 20-, and 24-mm cubes and rectangular prisms “ α ” through “ ι .”

5. Conclusions

The advection distance of any individual particle in a bore is the complex result of a number of factors, including particle orientation. Even when the same bore strikes the same particle in the same orientation, resulting advection distance can vary by up to 20%. The advection distance of particles with low shape factors varies significantly with initial orientation so that presenting the smallest face normal to the flow decreases advection distance and presenting the largest face normal to the flow increases it. The average behavior of large numbers of particles with mixed orientations, however, is more predictable, and appears not to depend on orientation but on size. Consequently, sediment-based paleohydraulic interpretations of tsunamis should use the behavior of many particles rather than one or two, and should attempt to use particles that might reasonably have been randomly oriented before advection.

6. References

- Blevins, R.D. (1984): *Applied Fluid Dynamics Handbook*. Van Nostrand Reinhold Co., Inc., New York, 558 pp.
- Dominey-Howes, D.T.M., G.A. Papadopoulos, and A.G. Dawson (2000): Geological and historical investigation of the 1650 Mt. Columbo (Thera Island) eruption and tsunami, Aegean Sea, Greece. *Nat. Hazards*, 21, 83–96.

- Makino, K. (1980): *Yaeyama no Meiwa otsunami [The great Meiwa tsunami in the Yaeyama Islands]*. Jyono Press, Kumamoto, Japan, 462 pp.
- Nakata, T., and T. Kawana (1993): Historical and prehistorical large tsunamis in the southern Ryukyus, Japan. *Tsunamis '93, Proceedings of IUGG/IOC Tsunami Symposium*, Wakayama, Japan, 297–307.
- Noji, M., F. Imamura, and N. Shuto (1985): Numerical simulation of movement of large rocks transported by tsunamis. *Proceedings of the IUGG/IOC International Tsunami Symposium*, Wakayama, Japan, 189–197.
- O'Brien, M.P., and J.R. Morison (1952): The forces exerted by waves on objects. *Trans. AGU*, 33, 32–38.
- Rouse, H.L. (1950): Fundamental principles of flow. In *Engineering Hydraulics*, edited by H.L. Rouse, Wiley, New York, 1–135.
- Simpkin, T., and R.S. Fiske (1983): *Krakatau, 1883—The Volcanic Eruption and its Effects*. Smithsonian Institution Press, Washington, D.C., 464 pp.
- Yamashita, B. (1995): The great Meiwa Sanriku tsunami [in Japanese]. NHK, 45 pp.
- Yeh, H.H., et al. (1993): The Flores Island tsunamis. *Eos Trans. AGU*, 74, 371–373.